Dynamics and Kinetics Study of "In-Water" Chemical Reactions by Enhanced Sampling of Reactive Trajectories

ARTICLE *in* THE JOURNAL OF PHYSICAL CHEMISTRY B · OCTOBER 2015

Impact Factor: 3.3 · DOI: 10.1021/acs.jpcb.5b08690

4 AUTHORS:

Jun Zhang

Peking University

6 PUBLICATIONS **1** CITATION

SEE PROFILE

Yi Isaac Yang

University of Lugano

8 PUBLICATIONS **4** CITATIONS

SEE PROFILE

Lijiang Yang

Peking University

39 PUBLICATIONS **822** CITATIONS

SEE PROFILE

Yi Qin Gao

Peking University

98 PUBLICATIONS **2,015** CITATIONS

SEE PROFILE

THE JOURNAL OF PHYSICAL CHEMISTRY B

Article

pubs.acs.org/JPCB

Dynamics and Kinetics Study of "In-Water" Chemical Reactions by Enhanced Sampling of Reactive Trajectories

Jun Zhang,[†,‡] Y. Isaac Yang,[†] Lijiang Yang,[†,‡] and Yi Qin Gao*[,†,‡]

[†]Institute of Theoretical and Computational Chemistry, College of Chemistry and Molecular Engineering, Peking University, Yiheyuan Road No. 5, Beijing 100871, China

[‡]Biodynamic Optical Imaging Center, Peking University, Beijing 100871, China

Supporting Information

ABSTRACT: High potential energy barriers and engagement of solvent coordinates set challenges for in silico studies of chemical reactions, and one is quite commonly limited to study reactions along predefined reaction coordinate(s). A systematic protocol, QM/MM MD simulations using enhanced sampling of reactive trajectories (ESoRT), is established to quantitatively study chemical transitions in complex systems. A number of trajectories for Claisen rearrangement in water and toluene were collected and analyzed, respectively. Evidence was found that the bond making and breaking during this reaction are concerted processes in solutions, preferentially through a chairlike configuration. Water plays an important dynamic role that helps stabilize the transition sate, and the dipole−dipole interaction between water and the solute also lowers the transition barrier. The calculated rate coefficient is consistent with the experimental measurement. Compared with water, the reaction pathway in toluene is "narrower" and the reaction rate is slower by almost three orders of magnitude due to the absence of proper interactions to stabilize the transition state. This study suggests that the "in-water" nature of the Claisen rearrangement in aqueous solution influences its thermodynamics, kinetics, as well as dynamics.

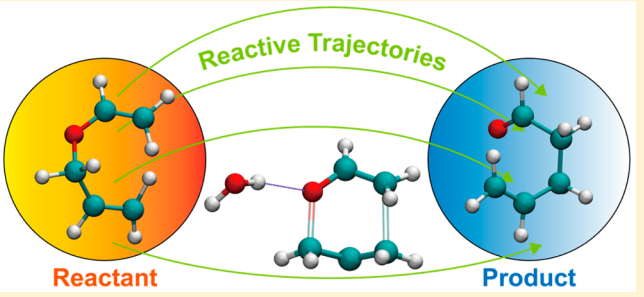

INTRODUCTION

When an enhanced sampling method using an effective Hamiltonian is implemented in a simulation, a problem emerges on how to retrieve the dynamics (and/or kinetics) information. To meet this challenge, it is compelling to acquire as much knowledge as possible about the transition pathways, which are usually embedded in a very complex energy landscape but critical for our understanding of the chemical kinetics; however, as is often the case, to drive the system through the transition paths is a nontrivial task because the transition process as in chemical reactions usually involves high free-energy barriers. Free-energy-based methods, for example, the metadynamics[1] and umbrella sampling[2] method, are useful in tackling chemical reactions with well-defined reaction coordinate(s) as a prior knowledge. Instead of directly calculating the kinetics of the system, these methods usually relate the rate constant to the activation energy along a certain reaction coordinate, although it could be difficult to find proper low-dimensional collective variables to describe the chemical reactions in complex environments. To focus on the kinetics, several methods have been devised to effectively search for the transition paths, including string method,[3] nudged elastic band,[4] mile-stoning, weighted-ensemble,[5] and forward flux[6] sampling method. Nevertheless, difficulties still exist to obtain the kinetics of a chemical reaction with the previously mentioned methods, despite the fact that the estimation of the rate constant according to the transition-state theory is possible if the minimum free energy pathway is known.

Another useful approach for sampling reactive trajectories is the transition path sampling (TPS) proposed by Chandler and coworkers.[7] In TPS, an initial trajectory connecting the reactant and the product can be obtained by way of, for instance, targeted molecular dynamics or high-temperature simulations. Starting from the initial trajectory, an ensemble of trajectories is generated by a shooting and shifting Monte Carlo procedure, which represents the transitions between the reactant and the product. Noticeably, the procedure of TPS ensures the authenticity of the dynamics of the system and it in principle requires no prior knowledge of reaction coordinates. A few variations of TPS have been proposed to further improve the computational efficiency, such as the transition interface sampling (TIS)[8] and its extension, the partial path TIS (PPTIS).[9] To obtain the reaction rate, the probability of finding successful reacting trajectories needs to be calculated. This step is usually done with a flux calculation executed separately, which is generally difficult to converge.

It thus remains highly desirable to further develop methods to efficiently sample important reaction pathways and calculate

Received: September 6, 2015
Revised: October 19, 2015

DOI: 10.1021/acs.jpcb.5b08690
J. Phys. Chem. B XXXX, XXX, XXX−XXX

the rate constant, overcoming the limitations and difficulties associated with preselecting reaction coordinate(s). We aim to obtain quantitative information on reaction mechanisms independent of initial structure input and improve the predicting power of computer simulations. In previous work, selective integrate-overtemperature (SITS) method has been demonstrated to exhibit great capability in searching the active phase space of a target chemical compound.[10−13] In this article, the efficiency of SITS for sampling chemical transitions is further improved. We present an approach that takes advantage of both SITS and TPS[10] to enhance the sampling of the reactive trajectories and calculate the reaction rate. For convenience, this approach is hereafter called after its main function: the enhanced sampling of reactive trajectories (ESoRT).

We implemented ESoRT in a QM/MM study of "in-water" Claisen rearrangement,[14] focusing on the understanding of the widely reported water-acceleration effect[15,16] on this reaction. For comparison, we also performed ESoRT on the same reaction but in a different solvent, toluene, also at 300 K and 1 atm. It was conventionally accepted that the reactant in this [3,3]-sigmatropic reaction, for example, allyl vinyl ether (AVE), was highly hydrophobic and thus poorly soluble in water. Hence the choice of solvents for this reaction was limited to nonpolar or weakly polar ones; however, after the 1980s, several organic reactions in which the reactant was hydrophobic were reported to be substantially accelerated in aqueous solutions, and Claisen rearrangement was found to be one outstanding example.[14,15] Over the past two decades, many computational efforts including ab initio quantum method and QM/MM MC/MD have been taken to explain such an unexpected phenomenon in Claisen rearrangement.[17−22] One popular postulation was that the hydrogen-donating capacity of water molecules (analogous to Lewis acid catalysis) would destabilize the ground state and stabilize the TS.[21−23] Additionally, some research indicated the large polarity of water might contribute to stabilizing the TS as well.[18] Because of limitations of computational efficiency, most of these simulations were initiated from a prerefined structure; then, the transition state (TS) was defined according to the intrinsic reaction coordinates (IRCs).[17,18] Challenges remain to investigate to what extent the thermodynamic and kinetic properties obtained on the basis of predefined reaction coordinates represent the true molecular mechanism of the reaction. On the contrary, to calculate the rate constant of chemical reactions by explicitly taking account of bulk solvent (which means the inclusion of solvent coordinates) and without merely following empirically predefined reaction coordinate(s), one has to deal with a large number of degrees of freedom.

The stereochemistry of the reaction under study has also been investigated by both experiments and computation, but the documented experiments were limited to substituted AVE molecules (which yield two chiral carbon sites in the product),[24,25] while in theoretical studies it has been difficult to take into account explicitly the effects of the complex solvation environment. ESoRT is featured by its ability to obtain unbiased and detailed information on chemical transitions (for example, the stereochemistry of chemical transitions and solvent effects), thus providing complementary and predictive knowledge to the experimental measurements. This selective enhancement of reactive trajectory sampling increased the efficiency in quantitatively describing the reaction pathways, yielding rate constants without the usage of predefined reaction coordinates, with a relatively low computational cost.

METHODS

The Hamiltonian $\mathbf{H}_t$ for the simulation system contains three terms as in eq 1,[26] where $\mathbf{H}_{QM}$ is for the QM-treated region, $\mathbf{H}_{MM}$ is for the MM-treated region, and $\mathbf{H}_{QM/MM}$ for the interaction between the two regions.

$$\hat{\mathbf{H}}_t = \hat{\mathbf{H}}_{QM} + \hat{\mathbf{H}}_{QM/MM} + \hat{\mathbf{H}}_{MM} \quad (1)$$

In our model system, the solvent is treated with molecular mechanics. The reactant (AVE) is treated with quantum mechanics, with no covalent bonds crossing the QM−MM boundary. In principle, SITS supports all quantum methods available in the hybrid MD. We chose the self-consistent charge density functional tight-binding (SCC-DFTB)[27,28] to quantify the potential energy of the reactant molecule. SCC-DFTB is computationally extremely efficient compared with the first-principle methods, while it generally ensures a reasonably good accuracy and has been shown to perform well in polar systems.[29] Over the past decade parameters in SCC-DFTB, especially those for elements including C, O, N, and H, were extensively benchmarked and widely applied in calculations involving organic compounds, biomolecules, and materials and gave reliable results.[30−32] Therefore, SCC-DFTB hopefully provides trustable description of the AVE molecule, which simply consists of those best-tested elements. Besides, we chose DFTB method also out of the consideration that it is always being systematically improved. The newly issued DFTB (to the third order) method[33] may provide even more accurate results in the future study of chemical reactions.

SITS is employed in the QM/MM MD[11,13] to enhance the sampling over the phase space of interest (i.e., the QM-treated region) and meanwhile keep the environment (MM-treated region) largely unperturbed. This strategy works by introducing a rescaled potential energy surface (eq 2)

$$U_{eff} = E_{MM} - \frac{1}{\beta_0} \ln \sum_k n_k e^{-\beta_k (E_{QM} + E_{QM/MM})} \quad (2)$$

in which U_{eff} is the effective potential; E_{MM}, E_{QM}, and $E_{QM/MM}$ stand for the energy of MM region, QM region, and QM/MM interaction, respectively; β_0 and β_k represent Boltzmann factors at temperature T_0 (namely, the target temperature) and T_k, respectively (T_k is a series of temperatures ranging from low to high, see later); and n_k values are weighting factors obtained through an iterative procedure.[34] As seen in eq 2, SITS is a potential-energy-based enhanced sampling method, and it integrates into the final effective PES with k PESs over a spread of k different temperatures simultaneously, among which the high-temperature ones are used to efficiently realize transitions across high-energy barriers while the statistical information near the simulation temperature (e.g., 300 K in this paper) can also be captured and maintained. After applying SITS to the simulation system, the QM part is able to reach a wide potential energy range that is essential for chemical reactions to occur; meanwhile, the remaining environment (MM-treated, e.g., solvents or enzymes) can be kept the least perturbed. Therefore, SITS-based methods including ESoRT are quite suitable for the study of chemical processes taking place at room temperature with complex environment, particularly the solution reactions and enzymatic reactions. The reweighting procedure is similar to that of standard SITS

DOI: 10.1021/acs.jpcb.5b08690
J. Phys. Chem. B XXXX, XXX, XXX−XXX

(which returns a weighting factor, w_{sits}) except for an extra term (w_{res}, see more details in the Supporting Information) accounting for the restriction (eq 3).

$$w = w_{sits} \cdot w_{res} = \frac{e^{-\beta_0[E_{QM}+E_{QM/MM}+E_{res}]}}{\sum_k n_k \cdot e^{-\beta_k[E_{QM}+E_{QM/MM}]}} \quad (3)$$

In eq 3, E_{res} represents the restraint energy that generates a Woods−Saxon-form force to help focus sampling on the reactive species (see more details in the Supporting Information), while other terms are the same as in eq 2. The standard procedure of ESoRT is given as follows. We first perform SITS QM/MM MD simulations to identify the active phase space of AVE. The conformational space of AVE was well-sampled and previously documented.[13] In the current paper, the rare event, namely, the transition process, is the priority for our sampling effort. Trajectory shooting is then executed in an NVE ensemble starting from the configurations sampled by the SITS simulation but using the original (unbiased) potential energy surface. These calculations give rise to both successful conversions, which turn a reactant to the product, and ones that remain as the reactant. We should note here that this latter calculation yields dynamics of the unbiased system and does not require predefined reaction coordinates except for the restraint. (See the Supporting Information.) Given that the statistical weight of each trajectory can be calculated at the desired temperature according to eqs 4 and 5, the rate constant of chemical reaction is obtained directly from the ratio between the weighted number of successful and that of all shot trajectories.

$$\eta = \frac{\sum_{suc} w_i}{\sum_{unsuc} w_i} \quad (4)$$

$$k = \left(\frac{\eta}{1+\eta}\right)/\tau = \frac{\sum_{suc\ traj} w_i}{\tau \sum_{all\ traj} w_i} \quad (5)$$

In eqs 4 and 5, η is the ratio between successful transitions and unsuccessful ones, w_i is the weighting factor of the corresponding initial configuration, which is obtained with eq 3, by replacing the two energy terms (i.e, E_{QM} and E_{res}) with the ones corresponding to the ith configuration (i.e., $E_{QM,i}$ and $E_{res,i}$, respectively), and τ here is the time for NVE shooting, namely, 2 ps.

SIMULATION DETAILS

One of the QM/MM MD systems was constructed in an aqueous and another in a toluene solution. We used periodic boundary conditions for both the water and toluene solvent box. In both systems, the reactant, ally vinyl ether (AVE), was treated with SCC-DFTB (see benchmark in the Supporting Information). In the MM-treated part, we used SPCE water model[35] for the water solvent molecules and the force field developed by Fox and Kollman for toluene.[36] The reactant first underwent a geometry optimization using Gaussian 09 (revision A.02)[37] and was assigned with RESP-A1A charges[38] by RED software package[39,40] before finally being fitted into AMBER-compatible force field parameters.[41] The concentration of the aqueous solution was ca. 0.09 mol/kg, which is below its saturation limit at room temperature.

The ESoRT MD simulations were executed on AMBER10 platform.[42] MD step was 1 fs. Each simulation system was first subjected to 500 steps of steepest descent energy minimization, followed by 2000 steps of conjugate gradient optimization. Then, a 50 ps MD was performed to heat the system up to 300 K, followed by another 50 ps MD to relax. To equilibrate the system to the appropriate volume, we adjusted the pressure of the system to 1 atm by the Berendsen weak-coupling algorithm[43] under another 1 ns long normal MD. After the equilibration step, a relative short (~5 ns) simulation for determining proper n_k (eqs 2 and 4) series for subsequent SITS-MD was performed using standard QM/MM MD simulation. The SITS QM/MM MD for sampling the reactive trajectories was performed by adopting an NTP ensemble at 1 atm and 300 K. The QM region was sampled by SITS. The temperatures used in eq 2 ranged from 220 to 1000 K with 150 sampling intervals. The transition path shootings on the unbiased potential energy surface were performed under NVE ensemble, each lasting for 2 ps. The time step for path shootings was again 1 fs. The preparation of transition path shootings and the analysis of the results are elaborated in the next section.

RESULTS

1. Enhanced Sampling of Reactive Trajectories: From Conformational Transitions to Chemical Transitions. As previously reported, there is a conformational equilibrium of AVE in aqueous solution.[13] The compact structures defined as those exhibiting a rather short C1−C6 distance (C1−C6 < 3.3 Å) are the prereactive species for the ensuing rearrangement of chemical bonds because such a [3,3]-sigmatropic reaction must undergo a 6-member-ring transition structure that originates from the compact conformers. Aiming at sampling the chemical transitions, we randomly selected an ensemble of compact structures to be the initial configurations for the following SITS simulations, with the statistical weight known from the SITS simulations. The representative set of initial configurations covered the entire compact conformation region (Figure S1), precluding any thermodynamics bias during selecting the prereactive conformers. As in the case of Claisen rearrangement (Scheme 1), since one bond is to form between C1 and C6 atoms and the other is to break between O3 and C4 atoms, trajectories in which C1 and C6 separate farther and O3 and C4 move closer are expected to not contribute to the reaction. To further increase the sampling of chemical reactions, we

Scheme 1. (a) Allyl Vinyl Ether (AVE) Underwent Claisen Rearrangement in Water Yielding 4-Pentenal and (b) Two-Step Mechanism Proposed for Aqueous Claisen Rearrangement, During Which the Reactant First Adopted a Proper Compact Conformation Then Reacted into the Product[a]

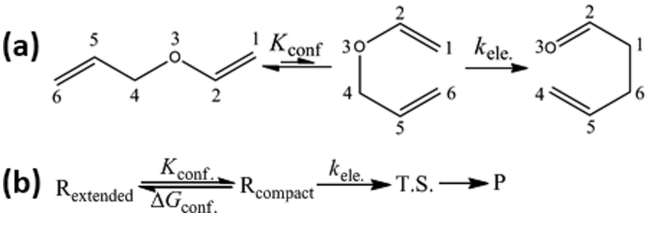

[a] $R_{extended}$ and $R_{compact}$ represent the extended and compact reactant molecules. T.S. and P denote for the transition state and product, respectively. K_{conf} and ΔG are the conformational equilibrium constant and the corresponding free energy. k_{ele} is the rate constant for the rate-limiting step (chemical-bond rearranging).

DOI: 10.1021/acs.jpcb.5b08690
J. Phys. Chem. B XXXX, XXX, XXX−XXX

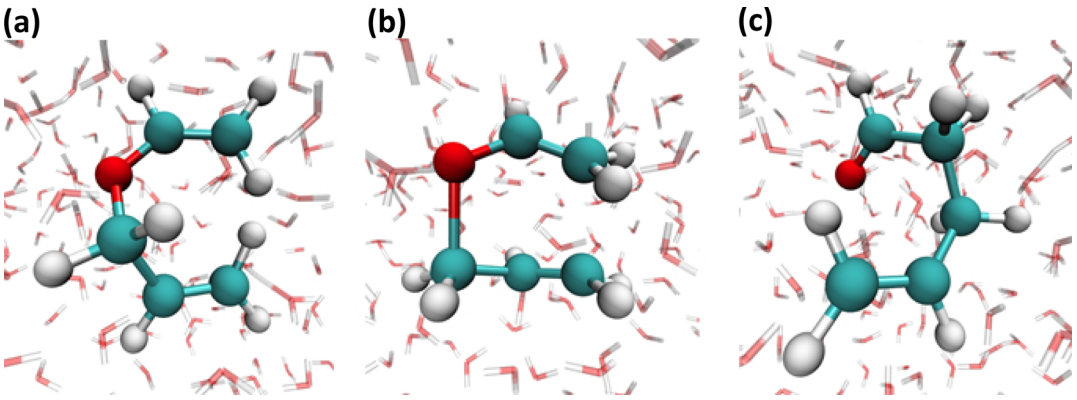

Figure 1. Snapshots during the chemical transitions: (a) the 6/7-member-ring compact reactant; (b) the 6-member-ring transition-state structure with lengthened O3−C4 bond and shortened C1−C6 distance; and (c) the product. Carbon atoms are rendered in cyan, oxygen in red, and hydrogen in white, respectively; the red-white triangles in the backdrop are water molecules.

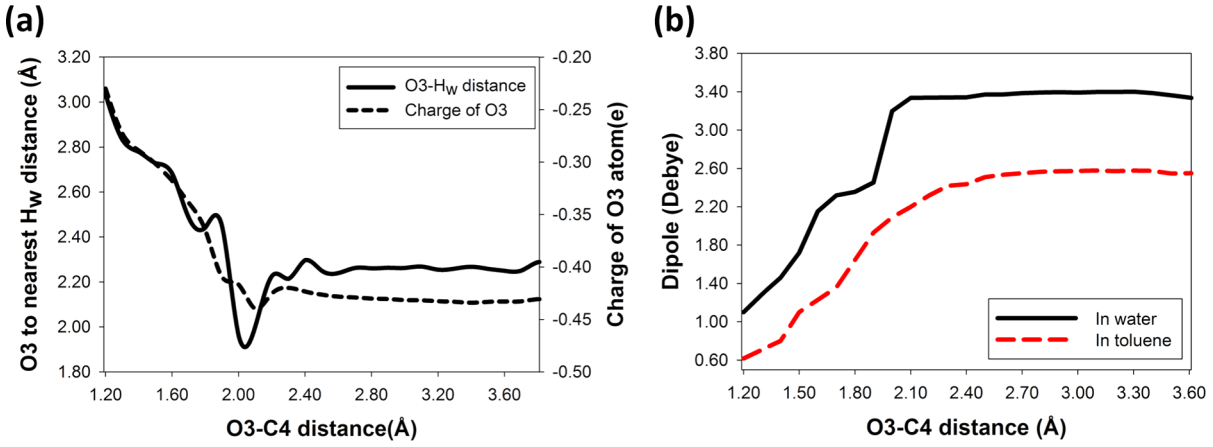

Figure 2. Analyses of the transition path ensemble. (a) Reaction proceeding is correlated with the hydrogen bond between water and AVE (solid line) and the electron density of O3 is related to the hydrogen-bond formation (dashed line). (b) Dipole moment of the reactant increases along the transition process as the O3−C4 bond is rupturing. The black solid line denotes the reaction in water and red dashed line corresponds to the reaction in toluene.

focus on the chemical transition but not the structural transformation between the compact and open structures, which is treated as a pre-equilibrium step. (See the details in the Supporting Information.)

Most of the AVE molecules among the ensemble of compact conformations selected above reacted into the desired product within 2 to 5 ns of the SITS-QM/MM MD simulations. (See an example movie in the Supporting Information.) Because the sampling of trajectories does not require predefined IRCs, the successful chemical transitions encompassed an ensemble of transition trajectories, along which configurations consistent with our common knowledge and intuition were observed (Figure 1, Figure S2).

We note here that in SITS simulations the system visited a broad energy range covering the reactant, T.S., and product, among which the low-energy species dominate and species of relatively high energy contribute little to the reweighted thermodynamics as a result of Boltzmann distribution. Compared with traditional TPS methods, ESoRT samples the phase space more thoroughly and hence enables the search of multiple pathways separated by high barriers because it avoids the entrapment of the trajectories in certain pathway(s). On the contrary, the energy required for the appearance of undesired byproducts would be generally too high for byproducts to play a significant role.

2. Analysis of the Reactive Transition Trajectories: Charge Polarization, Hydrogen-Bonding Effect, and Dipole−Dipole Interactions. An ensemble of transition paths containing more than 500 trajectories connecting the reactant (in the compact conformation) and product of Claisen rearrangement in the presence of solvent was obtained. These trajectories are registered as "reactive trajectories". These trajectories allowed us to investigate, in a statistical way, how water affects the chemical transition. From Figure 2a one sees that as the O3−C4 bond was rupturing, water donated hydrogen atoms to form hydrogen bonds with O3 of AVE. Strikingly, hydrogens of water interacted strongly with O3 of AVE when AVE was near the transition state (O3−C4 distance ~2.0 Å), with an H_{water}−O3 distance shorter than ordinary hydrogen bonds. This result, reminding one of the "hydrogen bonding effect" in water,[44] is in line with previous postulations over the catalytic mechanism of Lewis acids and BsCM enzymes on Claisen rearrangement and implies that the positive-charged atoms coordinating to O3 atom help stabilize the transition state.[21,45−47] Following this hypothesis, we correlated the Mulliken charge population on O3 atom with the bond breaking (Figure 2a). It was found that negative charges became enriched at O3 atom during Claisen rearrangement. In this reaction, the O3 atom turned from an sp^3 ether-oxygen to an sp^2-hybridized formyl-oxygen, and the electron

DOI: 10.1021/acs.jpcb.5b08690
J. Phys. Chem. B XXXX, XXX, XXX−XXX

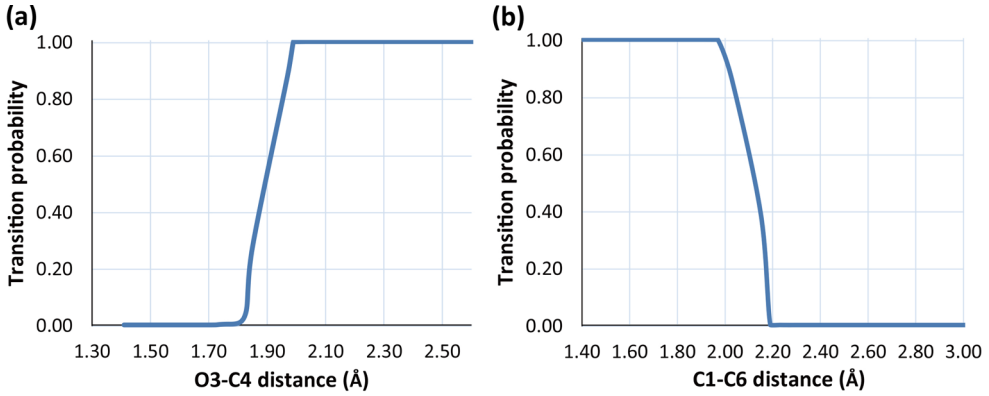

Figure 3. Committor analysis of the transition path ensemble and defining the reaction coordinates: (a) transition probability along the first dimension coordinate, O3−C4 distance (bond breaking sites), and (b) along the second dimension coordinate, C1−C6 distance (bond forming sites).

density reached a peak value when O3−C4 distance was between 1.9 and 2.0 Å. Thus, the hydrogen bond between water and O3 atom neutralizes part of the negative charge at O3 atom and stabilizes the transition state. This result reminds one of an old argument that the solvation effect of aqueous Claisen rearrangement was correlated with the hydrogen-donating capacity of water.[22,48] Our findings suggest a reasonable mechanism underlying such a correlation. Interestingly, O3 of the product tends to form a stronger hydrogen bond than the reactant, consistent with the fact that sp^2 O3 has a larger negative charge than sp^3 O3.

We also checked the effects of the dipolar medium on the transition process. The electrostatic properties of the T.S. of aliphatic Claisen rearrangement are still under debate.[22,49] Several computational studies claimed that Claisen rearrangement undergoes a dipolar transition state, and the dipole−dipole interactions between the T.S. and water solvent could serve to stabilize the T.S.[18] Our results showed that in water the dipole of AVE molecule increases from <1.5 to >3.0 D during the O3−C4 bond breakage. In consistency with previous results,[18,21] the transition state (with O3−C4 distance ∼1.9 to 2.0 Å) in water is more polar than the compact reactant, with an increase in dipole ($\Delta\mu = \mu_{T.S.} - \mu_{reactant}$) over 1.0 D (Figure 2b). It is noteworthy that this dipole moment of AVE consists of both the intrinsic and the induced dipole, and the solvent effect can be partly accredited to its role of enhancing the dipole−dipole interactions (including through the induced-dipole) between the solute and solvent. A similar but weaker tendency of dipole increase was also observed for this reaction in toluene. In contrast to water, toluene is a weak polar solvent and hence also weaker in its capability of inducing dipole (Figure 2b), indicating that water outperforms the nonpolar solvents in stabilizing the T.S. through dipole−dipole interactions.

3. Transition Path Shootings: Committor Analysis and Reaction Coordinates. In reference of the transition path sampling,[7,10] the rate constant calculation of chemical reactions requires shooting from the initial phase space points representing the Boltzmann distribution of the reactant and collecting the successful conversions. The ratio between the number of successful conversions and that of all trajectories within a given length of time can be used to calculate the desired rate constant (eq 5). Such a calculation requires the initial configurations used in eq 5 to resemble only the reactant, and the product-like structures should be excluded from trajectory shooting. Here committor analysis[7] was conducted to seek for a reasonable boundary separating reactant-like configurations apart from product-like ones (i.e., the separatrix[7,50−52]). By convention, C1−C6 and O3−C4 distances were chosen to be the coordinates[19,53] for committor analysis. The committor denotes the probability of a successful chemical transition beginning with certain initial O3−C4 distance or C1−C6 distance. The initial structure is more similar to the reactant if the committor is nearly zero and more alike the product when the committor takes a value close to 1.

About 500 initial structures (with recorded atomic coordinates, velocities, charges, as well as the effective weighting factors) were randomly selected from each reactive trajectory of the enhanced sampling simulation. The neighboring points were assured to be at least 0.5 ps apart in the SITS trajectories to reduce the correlation between the points generated by the same reactive trajectory. (See more details in the Supporting Information.) With these selected initial configurations, tens of thousands of MD trajectories, 2 ps each, were obtained on the original potential energy surface using an NVE ensemble. These trajectories, contain not only those that successfully arrived at typical product structures (i.e., a short C1−C6 length and a long O3−C4 distance) but also those that failed to do so. After reweighting the initial configurations, the committor at given O3−C4 distance or C1−C6 distance was obtained by eq 4.

As Figure 3 shows, almost all molecules starting with C1−C6 distance shorter than 2.0 Å or O3−C4 distance longer than 2.0 Å underwent a successful transition during the 2 ps NVE dynamic calculation. So we defined initial structures with C1−C6 > 2.1 Å and O3−C4 < 1.9 Å (which located near the midvalue point in the committor plot; see Figure 3) to be the representatives of reactant-like configurations. The sharp rise (or decline) in the committor plots shows that the corresponding nuclear coordinates are good reaction coordinates for depicting Claisen rearrangement.[54,55] Therefore, O3−C4 and C1−C6 distances were adopted hereinafter for the analyses of the transition state.

The final states of all these shootings were then judged to be the reactant or product, with the criterion derived from the committor analysis, (e.g., product was defined with C1−C6 distance shorter than 2.0 Å and O3−C4 distance longer than 2.0 Å). Finally, the rate constant k of this chemical transition process, through which the compact AVE transforms to 4-pentenal, was calculated using eqs 4 and 5.

DOI: 10.1021/acs.jpcb.5b08690
J. Phys. Chem. B XXXX, XXX, XXX−XXX

4. Convergence of ESoRT and the Rate Coefficient at 300 K under Aqueous Conditions. To examine the convergence of ESoRT, we calculated the rate constant using up to around 500 reactive trajectories. The details of ESoRT convergence are listed in Table S1. It can be seen that for the number of trajectories collected in this study the value of the rate coefficient has reasonably converged. As listed in Table S1, the rate at 300 K in water given by ESoRT $k_{ele}^{wat} = (2.2 \pm 0.6) \times 10^{-4}$ s^{-1}. It is noteworthy that this rate constant corresponds to the chemical bond rearrangement of the compact conformers during Claisen rearrangement. The overall rate constant of Claisen rearrangement of AVE in water should be the product of k_{ele} and the population of the compact conformation of the reactant in aqueous solution,[13] that is, K_{conf}, which is in the form of eq 6.

$$k_{overall} = \frac{K_{conf}}{K_{conf} + 1} k_{ele} \tag{6}$$

K_{conf} was reported to be 0.064 for AVE in water at 300 K,[13] so $k_{overall}^{wat} = (1.4 \pm 0.6) \times 10^{-5}$ s^{-1}. According to previous experimental measurements, the in-water reaction rate is estimated to be between 10^{-6} and 10^{-5} s^{-1}. (See more details in the Supporting Information.)

5. Solvation Effects on Activation Free Energy and Transition Pathway of Claisen Rearrangement. Using the rate constant calculated above and the transition-state theory rate equation, eq 7

$$k_{ele} = \frac{k_B T}{h} \exp\left(-\frac{\Delta G_{ele}^{\ddagger}}{RT}\right) = \frac{k_B T}{h} \exp\left(-\frac{\Delta H_{ele}^{\ddagger}}{RT} + \frac{\Delta S_{ele}^{\ddagger}}{R}\right) \tag{7}$$

where T is the temperature, k_B and h are Boltzmann and Planck constant, respectively, and one can estimate the activation free energy for the bond breaking/making step during Claisen rearrangement. The activation free energy for the chemical bond rearrangement in water (namely, $\Delta G_{ele}^{\ddagger}$) at 300 K is (22.6 ± 0.2) kcal/mol according to our calculations. Taking the conformational preadjustment[11,13] into account (in water ΔG_{conf} = 1.6 kcal/mol), the total $\Delta G^{\ddagger} \approx$ 24.2 kcal/mol, substantially lower than the value in the gas phase and nonpolar solvents, which was generally reported to be >28 kcal/mol, although different methods were used there.[56−58]

Because ESoRT does not require predefined coordinates to guide the reaction, it allows us to acquire information on visiting probabilities during the chemical transition and to obtain information about transition pathways using any postselected coordinate(s). (More features about ESoRT are discussed in the Supporting Information.) Conventionally, the bond length was used to describe the bond forming/breaking event. (See more details of choosing reaction coordinates in the Supporting Information.) Therefore, we projected the calculated visiting probabilities onto the distances between atoms at the bond forming (C1−C6) and breaking sites (O3−C4). Interestingly, the transition pathway of Claisen rearrangement in water is along the diagonal passage in Figure 4a, indicating that it is a concerted chemical reaction, in which the O3−C4 bond breaks with the C1−C6 bond forming simultaneously. The saddle point in the contour map representing the transition-state ensemble is located in the region near O3−C4−2.0 Å and C1−C6−2.1 Å, which is in good agreement with the committor analysis. Besides, Figure 4 shows that the C1−C6 bond shortens to ∼2.6 A before the O3−C4 bond stretches,

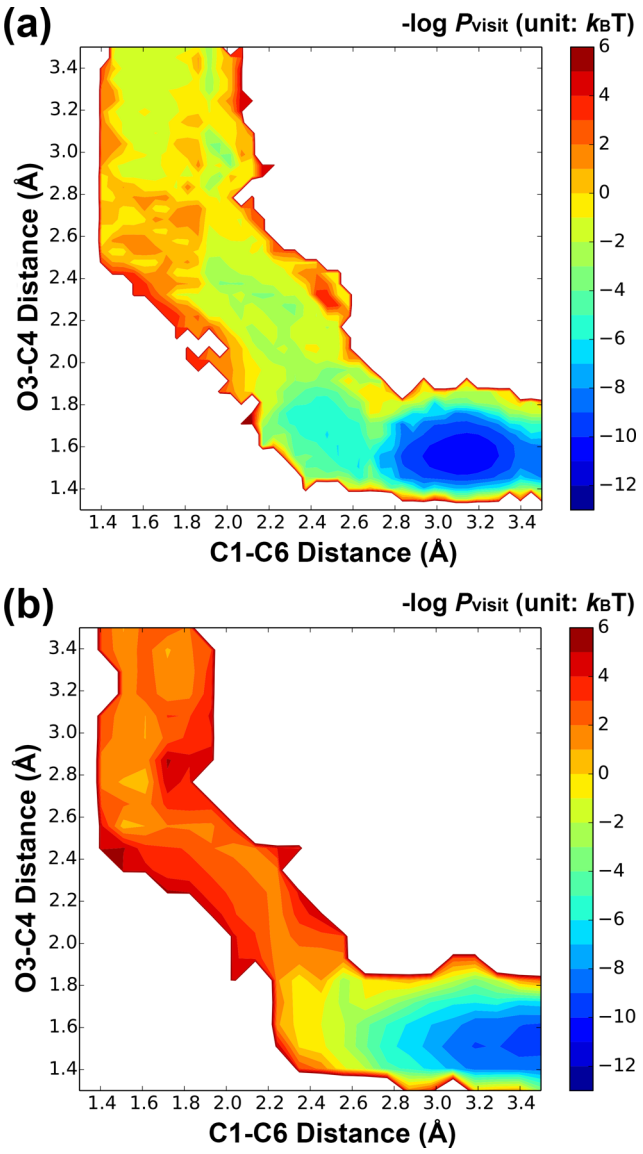

Figure 4. Contour map of transition pathways of AVE in water: (a) in water and (b) in toluene. The lower-right region with long C1−C6 distance and short O3−C4 distance represents the reactant, and the upper-left with long O3−C4 distance and short C1−C6 distance corresponds to the product. (Also see Scheme 1.) The landscape is rendered according to the minus logarithm of visiting probability of the configurations (−lg P_{visit}). Both pictures were drawn according to the NVE transition shootings, by projecting the visited configurations on to the 2D map and accumulating the corresponding weighting factors (which represent the occurrence probability of each trajectory under Boltzmann distribution).

consistent with the previous research defining the "reactive species" of AVE molecules, and it reflects the conformation preadjustment of reactant molecules in solution.

Following the standard ESoRT procedure (as applied in the AVE-water system), the rate coefficient of AVE reacting to 4-pentenal in toluene at 300 K was also obtained. The reaction rate in toluene was calculated to be $k_{ele}^{tol} = (1.1 \pm 0.8) \times 10^{-6}$ s^{-1}. Given the K_{conf} of AVE in toluene 9.2×10^{-3} (ΔG_{conf} = 2.8 kcal/mol),[13] the overall reaction rate in this widely used organic solvent was $k_{overall}^{tol} = 1.1 \times 10^{-8}$ s^{-1}, several thousand times smaller than that in water. In terms of activation free energy, compact AVE molecules encounter a $\Delta G_{ele}^{\ddagger}$ = 25.8 kcal/mol

DOI: 10.1021/acs.jpcb.5b08690
J. Phys. Chem. B XXXX, XXX, XXX−XXX

Scheme 2. Stereochemistry of Aliphatic Claisen Rearrangement[a]

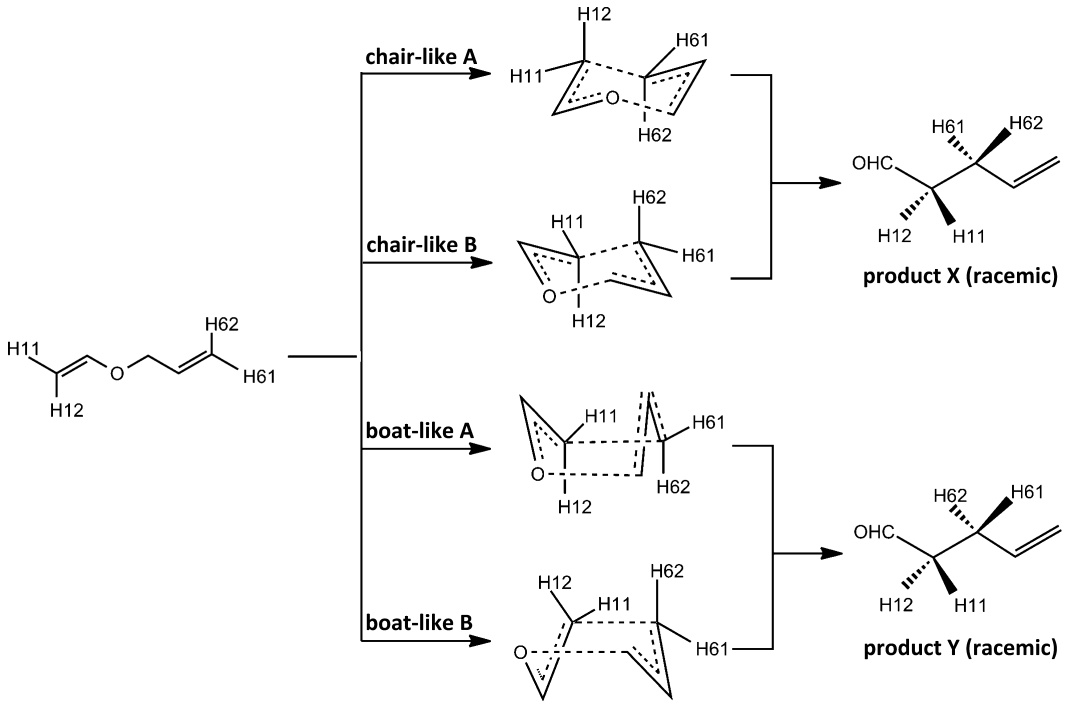

[a]Reactant AVE is inclined to undergo a chair-like T.S. (chair-like A and B) leading to the product X with specific chiral configuration and less likely to transform into product Y via boat-like (A and B) T.S. configurations.

energy barrier when undergoing Claisen rearrangement in toluene, which is ~3.2 kcal/mol higher than that in the aqueous solution. The overall activation free energy in toluene ($\Delta G^{\ddagger}$) is ca. 28.6 kcal/mol. These results are again consistent with experiment results and estimations.[48,56,58] We also projected all of the transition trajectories in toluene to the same reaction coordinates as selected for reactions in water (Figure 4b). It is clear that within the same iso-value boundary (e.g., $-\lg P_{visit}$ = 3.5) the transition path in toluene is narrower than that in water. This finding shows that water not only reduces the main barrier of the transition (namely the saddle point) but also broadens the free-energy transition pathway for AVE to react, indicating that the structure (or geometry) of the transition state is more variable and flexible in water than in toluene.

6. Geometry of T.S. The stereochemistry of Claisen rearrangement in the gas phase has been widely interrogated both experimentally and theoretically.[24,25,59,60] Experiments showed that the chairlike transition state was preferred during the [3,3]-sigmatropic reaction of 1,6-substituted AVE in the gas phase.[25] Computational evidence also supported that the chairlike geometry was adopted favorably during Claisen rearrangement,[61] although most of the calculations were limited to one preassumed configuration (e.g., the more stable chairlike one).[62] ESoRT allows a thorough configuration sampling, including the transitions via either a chairlike, a boat-like, or other noncanonical structures. Different from experiments, hydrogen atoms on the reactant in simulation can be labeled and thus distinguished from each other. AVE can react through two pairs of stochastically achiral transition states to provide two pseudoracemic diastereomers bearing newly generated centers of asymmetry at C2 and C3 of the products (Scheme 2). It therefore can pass through two enantiomeric chairlike transition states (named as chairlike A and B, respectively), both of which lead to the racemic diastereomer X. Similarly, the enantiomeric boat-like transition states evolve into racemic diastereomeric aldehyde Y. We calculated the proportion of chairlike transition structures in all of the successfully reacted NVE trajectories by analyzing the stereochemistry of C1 and C6 atoms in the products. (See more details in the Supporting Information.) The population ratio between racemic product 1 and racemic product 2 in water is ca. 10.8:1, giving the preference for a chairlike T.S. structure to be ~92% in aqueous solution. For AVE molecules bearing substituents on C1 and C6 atoms, experiments demonstrated that the chairlike T.S. dominates with a percentage of ~95%.[25,63] Our calculation showed that the T.S. for the parent AVE also prefers the chairlike configuration in water.

Additionally, it is intriguing to understand how solvents influence the stereochemistry of this reaction. Few computational studies have tackled this question because theoretical studies were commonly done with the usage of predefined reaction coordinates. By virtue of ESoRT, we can now compare the stereochemistry of Claisen rearrangement in different solvents. Interestingly, we found that the preference for a chairlike T.S. structure is >99% in toluene, a significant increase compared with the corresponding value in water (namely, 92%). It is well known that the dominance of chair-like over boat-like conformation for a six-member ring is due to the soothed unfavorable nonbonding interactions. The current study shows that the intramolecular interactions do vary in different solvents. Analyses of the transition pathways (Figure 4) provide an explanation for the observed difference. The broader transition path for AVE in water indicates that AVE adopts a looser transition state structure, and thus the 1−5 nonbonding interactions in boat-like configuration can be alleviated, leading to an increase in the boat-like T.S. population. Previous experimental studies did show that a more dipolar (or more charge-separated) T.S. induced by

DOI: 10.1021/acs.jpcb.5b08690
J. Phys. Chem. B XXXX, XXX, XXX−XXX

solvent, which was more tolerant for unfavorable nonbonding interactions, may lead to different stereoselectivity.[64,65] Inspired by this idea, we analyzed the charge separation of AVE molecule during the transition and found that water did induce a more charge-separated T.S. (Figure S3) than toluene did. Taking previous analyses of dipole moment together into consideration, these results suggest that the higher population of boat-like structure of T.S. in water is caused by the looser and more dipolar (more charge-separated) configuration of T.S.

DISCUSSION

1. Insight into Aqueous Acceleration Effect on Claisen Rearrangement. It has been documented that compared with the reaction in the gas phase, the Claisen rearrangement in aqueous solution observes a significant acceleration. Our simulations have shown that the solvent effect on such a widely used intramolecular pericyclic reaction caused by bulk water can be addressed from several respects. As proposed in our previous article,[13] Claisen rearrangement can be reschemed into a two-step kinetic process (Scheme 1b and Scheme 3). Thus, the overall free-energy barrier can be formulated by two major terms represented by eq 8 (see the derivation of eq 8 in the Supporting Information).

$$\Delta G^{\ddagger} = \Delta G_{\mathrm{conf}} + \Delta G^{\ddagger}_{\mathrm{ele}} \tag{8}$$

Scheme 3. Proposed Mechanism to Explain the Water-Acceleration Effect on Claisen Rearrangement[a]

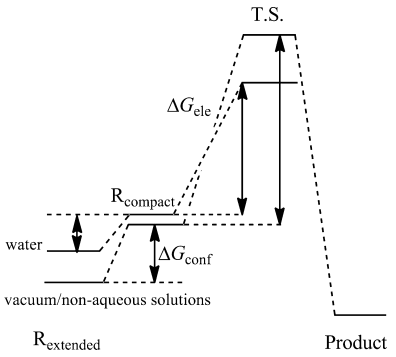

[a]Prior to the rate-limiting chemical transition, the bulk water helps accumulate the reactive compact conformation of the reactant. During the transition overcoming the high-energy barrier, water stabilizes the transition state by donating hydrogen bond(s) to the negatively charged atom(s) of the reactant and by other electrostatic forces such as dipole−dipole interactions.

First, the bulk water tends to accumulate the reactive compact conformation of AVE in water due to its strong cohesive interactions.[66] A smaller ΔG_{conf} observed for AVE in water than in other organic solvents can directly contribute to a smaller overall energy barrier and lead to a faster reaction rate k_{overall}.[13]

Second, the hydrogen-bond donating capability of water plays a key role in stabilizing the transition state of aliphatic Claisen rearrangement. AVE undergoes significant polarization and charge redistribution during C1−C6 bond formation and O3−C4 bond breaking. The transient negative charge of O3 reaches a peak value when the reactant approaches the transition state. Therefore, at the transition state, a stronger hydrogen bond forms between O3 and water to substantially reduce the energy of the electron rearrangement. Besides, the dipole−dipole interactions also serve to stabilize the transition state in aqueous solutions in contrast with in toluene or vacuum. All of these solvation effects lead to a significantly reduced $\Delta G^{\ddagger}_{\mathrm{ele}}$ and thus a smaller overall $\Delta G^{\ddagger}$ (Scheme 3). This scheme not only explains the acceleration of aqueous Claisen rearrangement but also provides a possible mechanism for other nontraditional in-water reactions.[15,67] Water can facilitate these in-water reactions from either the conformational adjustment or the chemical transition process or both. Investigation is being carried out in our group to explore such effects in other water-accelerated reactions including retro-Claisen rearrangement and Diels−Alder reactions.[15]

2. Solvent Effects on Transition Pathway and Transition-State Structure of Claisen Rearrangement. Solvent not only affects the energy barrier for the chemical transition (leading to an altered reaction rate) but also can profoundly influence the transition pathways and properties of transition state. According to our calculations, the transition passage of Claisen rearrangement in water is "broader" than that in toluene. This finding suggests that the reaction mechanism varies subtly in different solvents and the reaction coordinate is not completely determined by the reactant itself, and it should also include contributions from the solvent. Although the solvent molecules used in this work are empirically modeled (e.g., SPCE water), our results showed the importance of adequate consideration of solvent in the mechanism study of solution chemical reactions. Following this idea, an ongoing ab initio MD calculation with the catalytically important water molecules also being treated quantum mechanically is used to shed more light on the details of chemical reaction event such as the energy-transfer process during chemical bond breaking/forming.

In addition, we provided evidence showing that properties of the transition state are sensitive to the surroundings. Properties of the solvent can noticeably alter the properties of the transition state. For example, water as a strongly dipolar solvent induces a more dipolar T.S. compared with toluene, and meanwhile it allows a stronger charge separation within the T.S. during the reaction. Solvent effects may also cause differences in the geometry of the T.S., leading to different stereoselectivity of the synthetic product. As in Claisen rearrangement, the T.S. in aqueous solution appears more flexible than that in toluene, allowing for a higher chance of adopting the boat-like geometry and yielding a different stereochemical configuration of the product. As a consequence, the stereochemistry of the chemical reaction can be altered by the solvation environment.[68]

CONCLUSIONS

We established and tested a systematic methodology, ESoRT, to achieve enhanced sampling of the transition pathways and efficient calculations of rate constants for rare events for QM/MM studies of chemical reactions. ESoRT allowed the realization of in silico chemical transitions over high-energy barriers without being constrained to follow the predefined reaction coordinates. Besides, because of the biased sampling of the reactive region in the phase space, the convergence of transition path shootings was significantly accelerated. By implementing ESoRT in QM/MM MD simulations with explicit solvent, transitions of ally vinyl ether starting from the compact conformation into 4-pentenal in toluene and aqueous solutions were obtained. The rate constant calculated in water solution for the classic Claisen rearrangement of AVE into 4-pentenal is 1.4×10^{-5} s^{-1}, and the overall reaction rate in

DOI: 10.1021/acs.jpcb.5b08690
J. Phys. Chem. B XXXX, XXX, XXX−XXX

toluene turned out to be 1.1×10^{-8} s^{-1}, both of which are in agreement with the experimental measurement.

Making use of the representative configurations along the reactive trajectories, a thorough analysis of the reactive paths can be achieved for understanding the reaction and catalysis mechanism. It was shown that there is an accumulation of electron density at the heteroatom O3 during the bond forming/breaking process in the aqueous solution. The hydrogen bond between water and O3 at AVE, which could partially delocalize the negative charges, was found critical to stabilize the transition state. Besides, the dipole interactions between AVE and water also contributed to lower the transition barrier in the aqueous environment. Similar analysis revealed that these solvation effects became largely absent in toluene, as no hydrogen bond could form between toluene and AVE and the dipole−dipole interactions became significantly weakened. Therefore, the acceleration of aqueous Claisen rearrangement can be addressed from at least two aspects: (1) the enrichment of reactive compact conformation in the bulk water and (2) the stabilization of the transition state by the hydrogen bonding as well as the dipole−dipole interactions from nearby water. The calculations also showed that the chairlike configuration with less steric congestion is highly preferred for the transition state, particularly in the weakly/nonpolar solvent like toluene. Furthermore, Claisen rearrangement is shown to be a concerted process, while the transition path can be affected by the reaction environment, and thus the stereochemistry (and the stereoselectivity) of the reaction is also affected by the solvent used.

■ ASSOCIATED CONTENT

Supporting Information

The Supporting Information is available free of charge on the ACS Publications website at DOI: 10.1021/acs.jpcb.5b08690.

Details of the technical implementation of the methodology (ESoRT) and its convergence, with an example of chemical transition event without artificially chosen reaction coordinate. Estimation of reaction rate of in-water Claisen rearrangement from experimental measurements, which is used for comparison with our results. More extended topics around the new method ESoRT, ranging from its distinct features to the prospect of applications via ESoRT. Some properties of transition state, including the stereochemistry and the charge separation. Derivation of eq 8 in the main text and the benchmark of SCC-DFTB performance in our calculations. (PDF)

Example movie of chemical transition event without artificially chosen reaction coordinate. (AVI)

■ AUTHOR INFORMATION

Corresponding Author

*E-mail: gaoyq@pku.edu.cn.

Notes

The authors declare no competing financial interest.

■ ACKNOWLEDGMENTS

We thank the National Program on Key Basic Research Project (973 Program, No. 2012CB917304) and the Natural Science Foundation of China (91027044 and 21125311) for financial support.

■ REFERENCES

(1) Laio, A.; Parrinello, M. Escaping Free-Energy Minima. *Proc. Natl. Acad. Sci. U. S. A.* **2002**, *99*, 12562−12566.

(2) Torrie, G. M.; Valleau, J. P. Nonphysical Sampling Distributions in Monte Carlo Free-Energy Estimation: Umbrella Sampling. *J. Comput. Phys.* **1977**, *23*, 187−199.

(3) Weinan, E.; Ren, W.; Vanden-Eijnden, E. String Method for the Study of Rare Events. *Phys. Rev. B: Condens. Matter Mater. Phys.* **2002**, DOI: 10.1103/PhysRevB.66.052301.

(4) Mills, G.; Jónsson, H. Quantum and Thermal Effects in H_2 Dissociative Adsorption: Evaluation of Free Energy Barriers in Multidimensional Quantum Systems. *Phys. Rev. Lett.* **1994**, *72*, 1124.

(5) Huber, G. A.; Kim, S. Weighted-Ensemble Brownian Dynamics Simulations for Protein Association Reactions. *Biophys. J.* **1996**, *70*, 97.

(6) Allen, R. J.; Frenkel, D.; Ten Wolde, P. R. Simulating Rare Events in Equilibrium or Nonequilibrium Stochastic Systems. *J. Chem. Phys.* **2006**, *124*, 024102.

(7) Bolhuis, P. G.; Chandler, D.; Dellago, C.; Geissler, P. L. Transition Path Sampling: Throwing Ropes over Rough Mountain Passes, in the Dark. *Annu. Rev. Phys. Chem.* **2002**, *53*, 291−318.

(8) Moroni, D.; van Erp, T. S.; Bolhuis, P. G. Investigating Rare Events by Transition Interface Sampling. *Phys. A* **2004**, *340*, 395−401.

(9) Moroni, D.; Bolhuis, P. G.; van Erp, T. S. Rate Constants for Diffusive Processes by Partial Path Sampling. *J. Chem. Phys.* **2004**, *120*, 4055−4065.

(10) Fu, X.; Yang, L.; Gao, Y. Q. Selective Sampling of Transition Paths. *J. Chem. Phys.* **2007**, *127*, 154106.

(11) Yang, L.; Liu, C.-W.; Shao, Q.; Zhang, J.; Gao, Y. Q. From Thermodynamics to Kinetics: Enhanced Sampling of Rare Events. *Acc. Chem. Res.* **2015**, *48*, 947−955.

(12) Yang, L.; Gao, Y. Q. A Selective Integrated Tempering Method. *J. Chem. Phys.* **2009**, *131*, 214109.

(13) Zhang, J.; Yang, Y. I.; Yang, L.; Gao, Y. Q. Conformational Pre-Adjustment in Aqueous Claisen Rearrangement Revealed by SITS-QM/MM MD Simulations. *J. Phys. Chem. B* **2015**, *119*, 5518−5530.

(14) Grieco, P. A.; Brandes, E. B.; McCann, S.; Clark, J. D. Water as a Solvent for the Claisen Rearrangement: Practical Implications for Synthetic Organic Chemistry. *J. Org. Chem.* **1989**, *54*, 5849−5851.

(15) Chanda, A.; Fokin, V. V. Organic Synthesis "on Water. *Chem. Rev.* **2009**, *109*, 725−748.

(16) *Organic Synthesis in Water*; Grieco, P. A., Ed.; Springer: New York, 1998.

(17) Davidson, M. M.; Hillier, I. H.; Hall, R. J.; Burton, N. A. Effect of Solvent on the Claisen Rearrangement of Allyl Vinyl Ether Using ab initio Continuum Methods. *J. Am. Chem. Soc.* **1994**, *116*, 9294−9297.

(18) Gao, J. Combined QM/MM Simulation Study of the Claisen Rearrangement of Allyl Vinyl Ether in Aqueous Solution. *J. Am. Chem. Soc.* **1994**, *116*, 1563−1564.

(19) Sehgal, A.; Shao, L.; Gao, J. Transition Structure and Substituent Effects on Aqueous Acceleration of the Claisen Rearrangement. *J. Am. Chem. Soc.* **1995**, *117*, 11337−11340.

(20) Acevedo, O.; Armacost, K. Claisen Rearrangements: Insight into Solvent Effects and "on Water" Reactivity from QM/MM Simulations. *J. Am. Chem. Soc.* **2010**, *132*, 1966−1975.

(21) Severance, D. L.; Jorgensen, W. L. Effects of Hydration on the Claisen Rearrangement of Allyl Vinyl Ether from Computer Simulations. *J. Am. Chem. Soc.* **1992**, *114*, 10966−10968.

(22) Gajewski, J. J. The Claisen Rearrangement. Response to Solvents and Substituents: The Case for Both Hydrophobic and Hydrogen Bond Acceleration in Water and for a Variable Transition State. *Acc. Chem. Res.* **1997**, *30*, 219−225.

(23) Jung, Y.; Marcus, R. A. On the Theory of Organic Catalysis "on Water. *J. Am. Chem. Soc.* **2007**, *129*, 5492−5502.

(24) Vittorelli, P.; Winkler, T.; Hansen, H. J.; Schmid, H. Stereochemie Des Übergangszustandes Aliphatischer Claisen-Umlagerungen. Vorläufige Mitteilung. *Helv. Chim. Acta* **1968**, *51*, 1457−1461.

(25) Hansen, H.-J.; Schmid, H. Stereochemie von [3.3]-Und [5.5]-Sigmatropischen Umlagerungen. *Tetrahedron* **1974**, *30*, 1959−1969.

DOI: 10.1021/acs.jpcb.5b08690
J. Phys. Chem. B XXXX, XXX, XXX−XXX

(26) Senn, H. M.; Thiel, W. QM/MM Methods for Biomolecular Systems. *Angew. Chem., Int. Ed.* **2009**, *48*, 1198−1229.
(27) Elstner, M.; Porezag, D.; Jungnickel, G.; Elsner, J.; Haugk, M.; Frauenheim, T.; Suhai, S.; Seifert, G. Self-Consistent-Charge Density-Functional Tight-Binding Method for Simulations of Complex Materials Properties. *Phys. Rev. B: Condens. Matter Mater. Phys.* **1998**, *58*, 7260.
(28) Han, W. G.; Elstner, M.; Jalkanen, K.; Frauenheim, T.; Suhai, S. Hybrid SCC-DFTB/Molecular Mechanical Studies of H-Bonded Systems and of N-Acetyl-(L-Ala)-Methylamide Helices in Water Solution. *Int. J. Quantum Chem.* **2000**, *78*, 459−479.
(29) Otte, N.; Scholten, M.; Thiel, W. Looking at Self-Consistent-Charge Density Functional Tight Binding from a Semiempirical Perspective. *J. Phys. Chem. A* **2007**, *111*, 5751−5755.
(30) Elstner, M.; Jalkanen, K. J.; Knapp-Mohammady, M.; Frauenheim, T.; Suhai, S. Energetics and Structure of Glycine and Alanine Based Model Peptides: Approximate SCC-DFTB, AM1 and PM3Methods in Comparison with DFT, HF and MP2 Calculations. *Chem. Phys.* **2001**, *263*, 203−219.
(31) Gaus, M.; Cui, Q.; Elstner, M. Density Functional Tight Binding: Application to Organic and Biological Molecules. *Wiley Interdiscip. Rev. Comput. Mol. Sci.* **2014**, *4*, 49−61.
(32) Seifert, G.; Joswig, J. O. Density-Functional Tight Binding—an Approximate Density-Functional Theory Method. *Wiley Interdiscip. Rev. Comput. Mol. Sci.* **2012**, *2*, 456−465.
(33) Gaus, M.; Goez, A.; Elstner, M. Parametrization and Benchmark of DFTB3 for Organic Molecules. *J. Chem. Theory Comput.* **2013**, *9*, 338−354.
(34) Gao, Y. Q. Self-Adaptive Enhanced Sampling in the Energy and Trajectory Spaces: Accelerated Thermodynamics and Kinetic Calculations. *J. Chem. Phys.* **2008**, *128*, 134111.
(35) Berendsen, H.; Grigera, J.; Straatsma, T. The Missing Term in Effective Pair Potentials. *J. Phys. Chem.* **1987**, *91*, 6269−6271.
(36) Fox, T.; Kollman, P. A. Application of the RESP Methodology in the Parametrization of Organic Solvents. *J. Phys. Chem. B* **1998**, *102*, 8070−8079.
(37) Frisch, M.; Trucks, G.; Schlegel, H. B.; Scuseria, G.; Robb, M.; Cheeseman, J.; Scalmani, G.; Barone, V.; Mennucci, B.; Petersson, G. *Gaussian 09*, revision A. 02; Gaussian, Inc.: Wallingford, CT, 2009; p *200*.
(38) Bayly, C. I.; Cieplak, P.; Cornell, W.; Kollman, P. A. A Well-Behaved Electrostatic Potential Based Method Using Charge Restraints for Deriving Atomic Charges: The RESP Model. *J. Phys. Chem.* **1993**, *97*, 10269−10280.
(39) Vanquelef, E.; Simon, S.; Marquant, G.; Garcia, E.; Klimerak, G.; Delepine, J. C.; Cieplak, P.; Dupradeau, F.-Y. Red Server: A Web Service for Deriving RESP and ESP Charges and Building Force Field Libraries for New Molecules and Molecular Fragments. *Nucleic Acids Res.* **2011**, *39*, W511−W517.
(40) Dupradeau, F.-Y.; Pigache, A.; Zaffran, T.; Savineau, C.; Lelong, R.; Grivel, N.; Lelong, D.; Rosanski, W.; Cieplak, P. The Red. Tools: Advances in RESP and ESP Charge Derivation and Force Field Library Building. *Phys. Chem. Chem. Phys.* **2010**, *12*, 7821−7839.
(41) Allen, F. H.; Kennard, O.; Watson, D. G.; Brammer, L.; Orpen, A. G.; Taylor, R. Tables of Bond Lengths Determined by X-Ray and Neutron Diffraction. Part 1. Bond Lengths in Organic Compounds. *J. Chem. Soc., Perkin Trans. 2* **1987**, S1−S19.
(42) Case, D.; Darden, T.; Cheatham, T.; Simmerling, C.; Wang, J.; Duke, R.; Luo, R.; Crowley, M.; Walker, R. C.; Zhang, W. *Amber 10*; University of California: San Francisco, 2008.
(43) Berendsen, H. J.; Postma, J. P. M.; van Gunsteren, W. F.; DiNola, A.; Haak, J. Molecular Dynamics with Coupling to an External Bath. *J. Chem. Phys.* **1984**, *81*, 3684−3690.
(44) Butler, R. N.; Coyne, A. G. Water: Nature's Reaction Enforcer Comparative Effects for Organic Synthesis "in-Water" and "on-Water. *Chem. Rev.* **2010**, *110*, 6302−6337.
(45) Lutz, R. P. Catalysis of the Cope and Claisen Rearrangements. *Chem. Rev.* **1984**, *84*, 205−247.
(46) Dodziuk, H.; von Voithenberg, H.; Allinger, N. L. A Molecular Mechanics Study of Methyl Vinyl Ether an Related Compounds. *Tetrahedron* **1982**, *38*, 2811−2819.
(47) Lee, A.; Stewart, J. D.; Clardy, J.; Ganem, B. New Insight into the Catalytic Mechanism of Chorismate Mutases from Structural Studies. *Chem. Biol.* **1995**, *2*, 195−203.
(48) Gajewski, J. J. A Semitheoretical Multiparameter Approach to Correlate Solvent Effects on Reactions and Equilibria. *J. Org. Chem.* **1992**, *57*, 5500−5506.
(49) Martín Castro, A. M. Claisen Rearrangement over the Past Nine Decades. *Chem. Rev.* **2004**, *104*, 2939−3002.
(50) Klosek, M.; Matkowsky, B.; Schuss, Z. The Kramers Problem in the Turnover Regime: The Role of the Stochastic Separatrix. *Ber. Bunsenges. Phys. Chem.* **1991**, *95*, 331−337.
(51) Ryter, D. On the Eigenfunctions of the Fokker-Planck Operator and of Its Adjoint. *Phys. A* **1987**, *142*, 103−121.
(52) Ryter, D. Noise-Induced Transitions in a Double-Well Potential at Low Friction. *J. Stat. Phys.* **1987**, *49*, 751−765.
(53) Yoo, H. Y.; Houk, K. Transition Structures and Kinetic Isotope Effects for the Claisen Rearrangement. *J. Am. Chem. Soc.* **1994**, *116*, 12047−12048.
(54) Peters, B.; Trout, B. L. Obtaining Reaction Coordinates by Likelihood Maximization. *J. Chem. Phys.* **2006**, *125*, 054108.
(55) Peters, B. P. (TP|q) Peak Maximization: Necessary but Not Sufficient for Reaction Coordinate Accuracy. *Chem. Phys. Lett.* **2010**, *494*, 100−103.
(56) Schuler, F. W.; Murphy, G. W. The Kinetics of the Rearrangement of Vinyl Allyl Ether1. *J. Am. Chem. Soc.* **1950**, *72*, 3155−3159.
(57) Burrows, C.; Carpenter, B. K. Substituent Effects on the Aliphatic Claisen Rearrangements. 2. Theoretical Analysis. *J. Am. Chem. Soc.* **1981**, *103*, 6984−6986.
(58) Coates, R. M.; Rogers, B. D.; Hobbs, S. J.; Curran, D. P.; Peck, D. R. Synthesis and Claisen Rearrangement of Alkoxyallyl Enol Ethers. Evidence for a Dipolar Transition State. *J. Am. Chem. Soc.* **1987**, *109*, 1160−1170.
(59) Gill, G. The Application of the Woodward−Hoffmann Orbital Symmetry Rules to Concerted Organic Reactions. *Q. Rev., Chem. Soc.* **1968**, *22*, 338−389.
(60) Copley, S. D.; Knowles, J. R. The Uncatalyzed Claisen Rearrangement of Chorismate to Prephenate Prefers a Transition State of Chair-Like Geometry. *J. Am. Chem. Soc.* **1985**, *107*, 5306−5308.
(61) Wiest, O.; Black, K. A.; Houk, K. Density Functional Theory Isotope Effects and Activation Energies for the Cope and Claisen Rearrangements. *J. Am. Chem. Soc.* **1994**, *116*, 10336−10337.
(62) Dewar, M. J. S.; Healy, E. F.; Stewart, J. J. P. Location of Transition States in Reaction Mechanisms. *J. Chem. Soc., Faraday Trans. 2* **1984**, *80*, 227−233.
(63) Ziegler, F. E. The Thermal, Aliphatic Claisen Rearrangement. *Chem. Rev.* **1988**, *88*, 1423−1452.
(64) Ireland, R. E.; Mueller, R. H.; Willard, A. K. The Ester Enolate Claisen Rearrangement. Stereochemical Control through Stereoselective Enolate Formation. *J. Am. Chem. Soc.* **1976**, *98*, 2868−2877.
(65) Ireland, R. E.; Wipf, P.; Armstrong, J. D., III Stereochemical Control in the Ester Enolate Claisen Rearrangement. 1. Stereoselectivity in Silyl Ketene Acetal Formation. *J. Org. Chem.* **1991**, *56*, 650−657.
(66) Pirrung, M. C. Acceleration of Organic Reactions through Aqueous Solvent Effects. *Chem. - Eur. J.* **2006**, *12*, 1312−1317.
(67) Li, C.-J.; Chen, L. Organic Chemistry in Water. *Chem. Soc. Rev.* **2006**, *35*, 68−82.
(68) Lindström, U. M. Stereoselective Organic Reactions in Water. *Chem. Rev.* **2002**, *102*, 2751−2772.

DOI: 10.1021/acs.jpcb.5b08690
J. Phys. Chem. B XXXX, XXX, XXX−XXX